



ORIGINAL ARTICLE

Computational and electrochemical investigation for corrosion inhibition of nickel in molar sulfuric acid by dihydrazide derivatives. Part II



H. Shokry ^{a,*}, E.M. Mabrouk ^b

^a Chemistry Department, Faculty of Science, Kafr El-Sheikh University, Kafr El-Sheikh 33516, Egypt

^b Chemistry Department, Faculty of Applied Science, Umm-Al Qura University, Makah, Saudi Arabia

Received 7 May 2013; accepted 28 January 2014
Available online 5 February 2014

KEYWORDS

Corrosion;
Inhibitors;
Mulliken atomic charges;
Fukui indices

Abstract Correlation of the efficiency of some dihydrazide derivatives, namely malonic acid (MAD), succinic acid (SAD) and adipic acid (AAD) dihydrazide, against the corrosion of nickel in 1 M sulfuric acid solution is discussed using electrochemical polarization method and quantum chemical calculations based on the ab initio method. The quantum chemical parameters calculated are, the highest occupied molecular orbital (HOMO), the lowest unoccupied molecular orbital (LUMO), the gap energy (ΔE), the dipole moment (μ), the softness (σ) and the total energy (TE). The relations between the inhibition efficiency and some quantum parameters are discussed and correlations are proposed. The protection efficiencies of these compounds showed a certain relationship to Mulliken atomic charges and Fukui indices. Dihydrazide inhibitor (AAD) exhibited the highest inhibition efficiency.

© 2014 Production and hosting by Elsevier B.V. on behalf of King Saud University. This is an open access article under the CC BY-NC-ND license (<http://creativecommons.org/licenses/by-nc-nd/3.0/>).

1. Introduction

The protection of metal surfaces against corrosion is an important industrial and scientific topic. Inhibitors are one of the practical means of preventing corrosion, particularly in acidic media. Inhibitors can adhere to a metal surface to form a protective barrier against corrosive agents in contact with

metal. The effectiveness of an inhibitor to provide corrosion protection depends to a large extent on the interaction between the inhibitor and the metal surface. The adsorbed inhibitors can affect the corrosion reaction, either by the blocking effect of the adsorbed inhibitor on the metal surface or by the effects attributed to the change in the activation barriers of the anodic and cathodic reactions of the corrosion process. There has been a growing interest in the use of organic compounds as inhibitors for the aqueous corrosion of metals. The action of inhibition of nickel and its alloys in acidic media by various organic and inorganic inhibitors has been widely studied (Aksut and Bilgic, 1992; Frignani et al., 1998; Maayta and Rawshdeh 2004; Maitra and Bhattacharyya 1979; Zinola and Castro Luna 1995; Fouda et al., 2013; Khamis et al., 1991; Lewis, 1982; Schmit 1984; Feller et al., 1973; Graz and Galzer,

* Corresponding author. Tel./fax: +20403415540.

E-mail address: drheshokry@yahoo.com (H. Shokry).

Peer review under responsibility of King Saud University.



Production and hosting by Elsevier

1974; Barkalatsova and Pshenicknikov 1976; Kesten 1976; Rengamani and Lyer, 1993; Reshetnikov 1978; Mohammed et al., 2012). Organic compounds, which can donate electrons to unoccupied d orbitals of metal surface to form coordinate covalent bonds and can also accept free electrons from the metal surface by using their antibonding orbitals to form feedback bonds, constitute excellent corrosion inhibitors. The most effective inhibitors are those compounds containing heteroatoms like nitrogen, oxygen, sulfur and phosphorus (Abdallah et al., 2003). The inhibitory activity of these molecules is accompanied by their adsorption to the metal surface. Free electron pairs on heteroatoms or π electrons are readily available for sharing to form a bond and act as nucleophile centers of inhibitor molecules and greatly facilitate the adsorption process over the metal surface, whose atoms act as electrophiles. Recently, the effectiveness of an inhibitor molecule has been related to its spatial as well as electronic structure (Valdez et al., 2005; Stoyanova and Peyerimhoff, 2002; Gomez et al., 2006; Finsgar et al., 2008).

Quantum chemical calculations have been widely used to study reaction mechanisms (Tao et al., 2010). They have also been proved to be a very powerful tool for studying inhibition of the corrosion of metals (Emregul and Hayvali, 2006; Valdez et al., 2006; Khaled et al., 2005). It has been found that the effectiveness of a corrosion inhibitor can be related to its electronic and spatial molecular structure (Bentiss et al., 2007; Xia et al., 2008; Ebenso et al., 2010; Arslan et al., 2009; Hansch et al., 1979).

The aim of this work is to study the influence of three selected dihydrazides, namely malonic acid (MAD), succinic acid (SAD) and adipic acid (AAD) dihydrazide, against the

corrosion of nickel in molar sulfuric acid solution which is discussed using electrochemical polarization and quantum chemical calculations based on the ab initio with basis set STO-3G method. It was also the purpose of the present work to discuss the relationship between quantum chemical calculations and experimental protection efficiencies of the three tested inhibitors by determining various quantum chemical parameters. These parameters include the highest occupied molecular orbital (E_{HOMO}) and the lowest unoccupied molecular orbital (E_{LUMO}), the energy difference ($\Delta E = E_{\text{LUMO}} - E_{\text{HOMO}}$). The local reactivity has been analyzed by means of the Fukui indices (Yang and Mortier, 1986; Rodriguez-Valdez et al., 2005), since they indicate the reactive regions, in the form of the nucleophilic and electrophilic behavior of each atom in the molecule.

2. Experimental

The current–voltage characteristics are recorded with an EG&G potentiostat/galvanostat model 173 and digital potentiometer (D.P) type C.G.822. The detailed experimental procedure has been given elsewhere (Gatos, 1956). Nickel in the form of wire (99.99%) in the case of polarization measurements, was fixed in glass tubing, such that only a surface area of 0.3 cm² was exposed to 100 ml of the corrosive medium, a saturated calomel electrode and a platinum wire were used as reference and auxiliary electrodes, respectively. All chemicals used were of A.R quality. The solutions were prepared using twice-distilled water. The investigated dihydrazide derivatives have the following molecular structures:

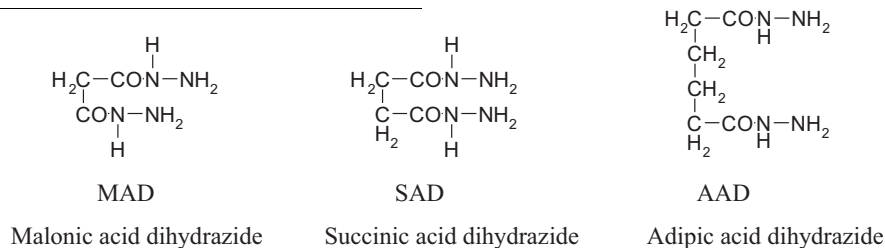


Table 1 Electrochemical parameters derived from polarization curves of nickel in 1 M H₂SO₄ at 30 °C.

Inhibitor	Conc., M	β_c , mV/current decade	β_a , mV/current decade	E_{corr} , mV (SCE)	i_{corr} (A.Cm ⁻²)	θ	H %
MAD	0.000	110	67	-217	22.2	-	-
	1×10^{-3}	172	69	-244	18.5	0.17	16.74
	5×10^{-3}	186	74	-234	14.3	0.31	31.14
	1×10^{-2}	180	69	-207	11.3	0.40	40.19
	5×10^{-2}	147	71	-197	7.7	0.69	63.83
	1×10^{-1}	135	70	-146	6.1	0.73	72.55
SAD	0.000	110	67	-217	22.2	-	-
	1×10^{-3}	175	69	-102	15.7	0.32	32.67
	5×10^{-3}	120	71	-221	11.2	0.50	49.78
	1×10^{-2}	117	75	-214	9.7	0.56	56.26
	5×10^{-2}	90	70	-280	8.5	0.82	61.93
	1×10^{-1}	84	72	-284	4.9	0.92	91.58
AAD	0.000	110	67	-217	22.2	-	-
	1×10^{-3}	174	75	-222	11.7	0.47	47.48
	5×10^{-3}	142	70	-190	7.8	0.65	64.99
	1×10^{-2}	125	75	-231	5.9	0.73	73.31
	5×10^{-2}	118	80	-220	4.6	0.79	79.16
	1×10^{-1}	138	77	-160	2.0	0.99	99.20

The inhibitive efficiency was calculated employing the formula:

$$\%IE = \left(1 - \frac{i_{inh}}{i_{free}}\right) \times 100 \quad (1)$$

where i_{free} and i_{inh} are the corrosion current densities without and with inhibitor, respectively. The surface coverage (θ) of the adsorbed inhibitors was calculated using the equation (Ateya et al., 1976):

$$\theta = \left(1 - \frac{i_{inh}}{i_{free}}\right) \quad (2)$$

3. Theoretical calculation

For quantum chemical calculations, the study was carried out using ab initio with basis set STO-3G method with commercially available quantum chemical software hyperchem release 7.5 for Widows (HyperChem™ Professional 2002) Molecular Modeling System. A full optimization of all geometrical variables without any symmetry constraint was performed at the Restricted Hartree-Fock (RHF) level (Wolinski et al., 1990; Dewar and Liotard, 1990). This develops the molecular orbitals on a valence basis set and also, calculates electronic properties, optimized geometries and total energy of the molecules. As an optimization procedure, the built-in Polak-Ribiere algorithm was used (Luenberger, 1973). Atomic Fukui indices, which are obtained from the electron density, are useful in predicting which atoms in a molecule are most likely to suffer nucleophilic, electrophilic, or radical attacks.

The local reactivity of the studied inhibitor molecules was analyzed through an evaluation of the Fukui indices (Yang and Mortier, 1986). These are a measurement of the chemical reactivity, as well as an indicative of the reactive regions and the nucleophilic and electrophilic behavior of the molecule. All calculations are done at the ground-state geometry. These functions can be condensed to the nuclei by using an atomic charge partitioning scheme, such as Mulliken population analysis. An easy graphical display technique can also be used based on the Fukui functions. Instead of calculating the molecular orbitals for the neutral, cation, and anion, we can just add or subtract electrons from the molecular orbitals of the neutral molecule. This procedure is not as good as described above, but it does give a quick graphical display of the susceptibility of different kinds of attack.

4. Results and discussion

4.1. Electrochemical measurements

Table 1 shows the corrosion rates and the % inhibition efficiencies of the present inhibitors in acid media. The corrosion rate of nickel for the blank solution 1 M H₂SO₄ is higher than those obtained for solutions containing various concentrations of inhibitors. This indicates that the corrosion of nickel in H₂SO₄ solution is inhibited by various concentrations of inhibitors.

From the calculated values of the inhibition efficiencies of tested inhibitors, it is indicative that these compounds inhibit the corrosion of nickel in the acid solution and their inhibition efficiencies decrease in the following trend, AAD > SAD > -

MAD. Fig. 1 shows the galvanostatic polarization curves of nickel in molar H₂SO₄ solution in the presence and in the absence of various concentrations of compound MAD as a typical example of these compounds. As can be seen, both the cathodic and the anodic reactions are inhibited and the inhibition increases as the inhibitor concentration increases, but the cathode is more polarized ($\beta_c > \beta_a$). Similar results were obtained for other tested compounds. Tafel line slopes were obtained as can be seen from Table 1. The order of decreasing inhibition efficiency was found to be: AAD > SAD > MAD.

The adsorption characteristics of the inhibitors were investigated by fitting the experimental data obtained for the degrees of surface coverage into different adsorption isotherms. The test data revealed that the adsorption of MAD, SAD and AAD can be described by the Langmuir adsorption isotherm. Several adsorption isotherms are attempted to fit the surface coverage, θ , including those of Frumkin, Temkin, Freundlich and Langmuir isotherms. For the studied inhibitors, it is found that the experimental data obtained from hydrogen evolution measurements, as an example of the other used experimental techniques, could fit the Langmuir's adsorption isotherm. According to this isotherm, the surface coverage (θ) is related to inhibitor concentration, C_{inh} , by the relation (Zhao and Mu 1999; Solmaz 2014; Dehri and Ozcan 2008; Deng 2011).

$$\frac{\theta}{1 - \theta} = K_{(ads)} C_{(inh)} \quad (3)$$

or

$$\frac{C_{(inh)}}{\theta} = \frac{1}{K_{(ads)}} + C_{(inh)} \quad (4)$$

and

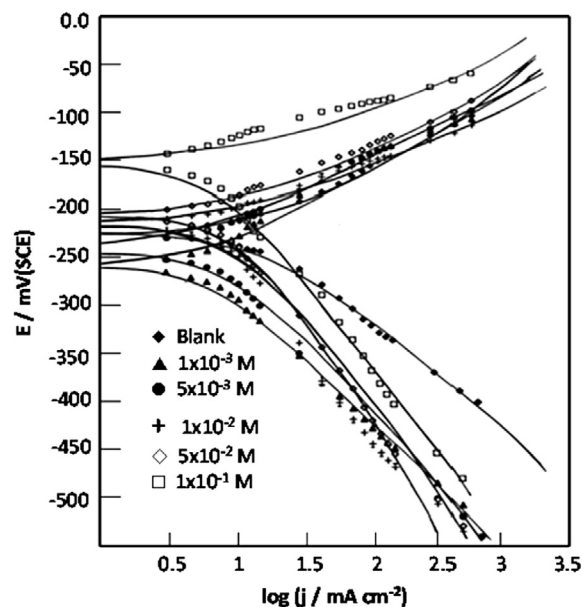


Figure 1 Polarization curves (I - E) of nickel in 1 M H₂SO₄ solution in the presence and in the absence of various concentrations of compound MAD.

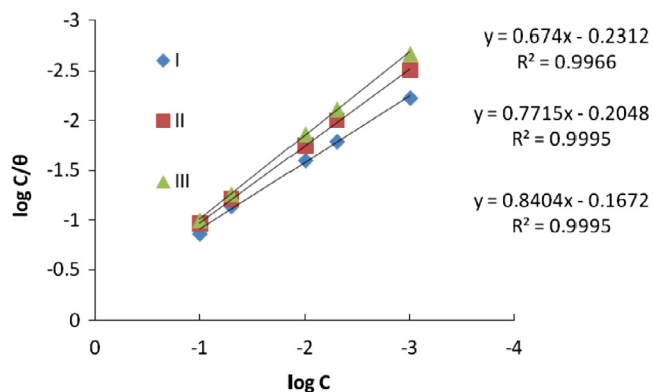


Figure 2 Langmuir adsorption Isotherm plots of inhibitors I (MAD), II (SAD) and III (AAD).

$$\log \left(\frac{C_{(inh)}}{\theta} \right) = \log C_{(inh)} - \log K_{(ads)} \quad (5)$$

Fig. 2 shows the plots of values of $\log(C/\theta)$ versus $\log C$. The plots were found to be linear indicating the application of the Langmuir isotherm to the adsorption of MAD, SAD and AAD on nickel surface. Values of adsorption parameters deduced from the Langmuir adsorption isotherms are presented in Table 2. The results obtained indicated that the $R^2 > 0.99$, as a strong correlation coefficient value, which value, signifies the strong adherence of inhibitors to the metal surface.

The values of the adsorption equilibrium constant K_{ads} obtained from the intercept of the Langmuir adsorption isotherms are related to the free energy of adsorption according to Eq. (6) (Eddy et al., 2009a,b; Quraishi et al., 2008).

$$\Delta C_{ads}^0 = -RT \ln(55.5 K_{ads}) \quad (6)$$

where ΔG_{ads}^0 is the free energy of adsorption, R is the gas constant and T is the absolute temperature of the system.

Generally, if the values of ΔG_{ads}^0 are in the range up to -20 kJ/mol, they are consistent with physisorption of the organic molecules or their protonated species on the surface. Inhibition is, therefore, due to electrostatic interaction between charged species and the charged metal, while those above -40 kJ/mol are associated with chemisorption as a result of sharing or transfer of electrons from organic species to the metal surface to form a metal bond (Gurten et al., 2007; Solomon et al., 2010). The calculated values of the standard free energy of reaction, ΔG_{ads}^0 , in this study (Table 2) the value is between -5.1 and -6.4 kJ/mol. This indicates that the adsorption mechanism of all the used inhibitors on nickel in 1 M H_2SO_4 solution is through physisorption (adsorptive film with an electrostatic character). The values of ΔG_{ads}^0 decrease in the

Table 2 Langmuir parameters for the adsorption of MAD, SAD and AAD on nickel surface, at 30 °C.

Inhibitor	intercept	ΔG^0 (kJ mol ⁻¹)	R^2
MAD	0.2312	-6.426	0.9966
SAD	0.2048	-6.121	0.9995
AAD	0.1672	-5.160	0.9995

order: AAD > SAD > MAD which reflects their tendency to inhibit the corrosion of Ni in 1 M H_2SO_4 solutions.

4.2. Quantum chemical calculation

Quantum chemical methods have already proven to be very useful in determining the molecular structure as well as elucidating the electronic structure and reactivity (Kraka and Cremer, 2000). Thus, it has become a common practice to carry out quantum chemical calculations in corrosion inhibition studies. The concept of assessing the efficiency of a corrosion inhibitor with the help of computational chemistry is to search for compounds with desired properties using chemical intuition and experience into a mathematically quantified and computerized form. Once a correlation between the structure and activity or property is found, any number of compounds, including those not yet synthesized, can be readily screened employing computational methodology (Karelson et al., 1996) and a set of mathematical equations which are capable of representing accurately the chemical phenomenon under study (Hinchliffe, 1994; Hinchliffe, 1999).

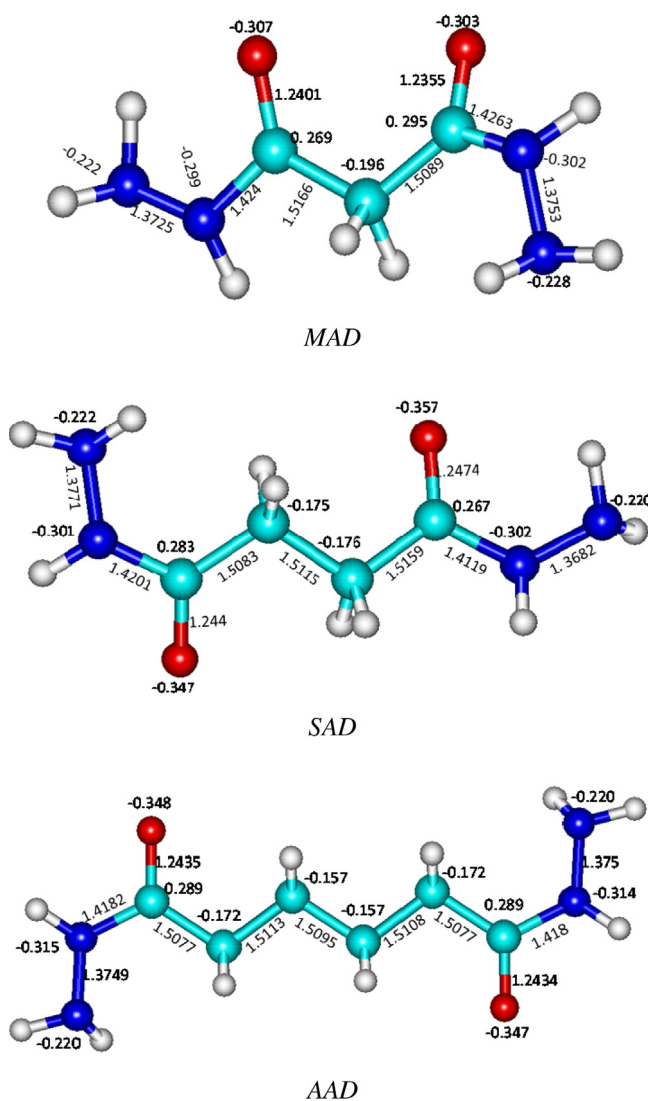


Figure 3 The optimized molecular structure of the inhibitor molecules MAD, SAD and AAD.

Geometric and electronic structures of the tested inhibitors are calculated by the optimization of their bond lengths, bond angles and charges. The optimized molecular structures with minimum energies obtained from the calculations are given in Fig. 3.

It is shown from the calculation of geometrical structure of dihydrazide compound that longest bonds are N—N and C=O with bond lengths ≈ 1.3749 and 1.2434 Å respectively, which can facilitate the adsorption of dihydrazide molecule on the metal surface through the N—N and C=O bonds. This is confirmed from the calculation of their bond order, 0.9867 and 1.796, which show weak bond character, and accordingly, the adsorption of the inhibitor on the metal surface becomes easier. The calculated charges show negative charges on N and O atoms, ≈ -0.222 e and -0.347 e, respectively, which can be considered as the active centers for the adsorption of dihydrazide molecule on the metal surface. The charge distribution over the whole skeleton of the molecule is shown in Fig. 3.

Table 3 shows the values of some quantum chemical parameters, namely the energy of the highest occupied molecular orbital (E_{HOMO}), energy of the lowest unoccupied molecular orbital (E_{LUMO}), the energy gap ($\Delta E = E_{\text{LUMO}} - E_{\text{HOMO}}$), (Bouklah et al., 2005; Martinez et al., 2007; Pang et al., 2007; Şahin et al., 2008) the total electronic energy of the molecules (TE), dipole moment (μ), substituent constant ($\log P$) which measures the differential solubility of a compound in two solvents and characterizes the hydrophobicity/hydrophilicity of a molecule, molecular polarizability (Pol), molecular volume (V_m), molecular surface area or solvent accessible molecular surface area (Ar) and the softness (σ).

The inhibition effect of inhibitor compound is usually ascribed to adsorption of the molecule on metal surface. There can be physical adsorption (physisorption) and chemical adsorption (chemisorption) depending on the adsorption strength. When chemisorption takes place, one of the reacting species acts as an electron pair donor and the other one acts as an electron pair acceptor, so the energies of the frontier molecular orbitals should be considered. The reactive highest occupied molecular orbital (HOMO) and lowest unoccupied molecular orbital (LUMO) of any molecule are referred to as frontier molecular orbitals, after the pioneering work of Fukui (Fukui et al., 1954).

The HOMO is the orbital that could act as an electron donor, since it is the outermost (highest energy) orbital containing electrons. The LUMO is the orbital that could act as the electron acceptor, since it is the innermost (lowest energy)

orbital that has room to accept electrons. According to the frontier molecular orbital theory, the formation of a transition state is due to an interaction between the frontier orbitals (HOMO and LUMO) of reactants (Issa et al., 2008). The energy of the HOMO is directly related to the ionization potential and the energy of the LUMO is directly related to the electron affinity.

Highest occupied molecular orbital energy (E_{HOMO}) and lowest unoccupied molecular orbital energy (E_{LUMO}), also called the frontier orbitals determine the possibility of the molecule to interact with other reactants. E_{HOMO} is often a measure of electron donating ability of the molecule. High value of E_{HOMO} is likely to indicate a tendency of the molecule to donate electrons to an appropriate acceptor molecule of low empty molecular orbital energy. The energy of the lowest unoccupied molecular orbital, E_{LUMO} , denotes the ability of the molecule to receive electrons. In other words, lower values of E_{LUMO} , are more probable to accept electrons. So, the gap energy, i.e. the difference in energy between the HOMO and LUMO, is an important stability index.

In our study, values of HOMO energy may be a good tool to interpret the efficiency of dihydrazide obtained. The calculations show that the MAD, SAD and AAD are the highest HOMO levels at -10.64 , -10.141 and -9.641 eV, respectively;

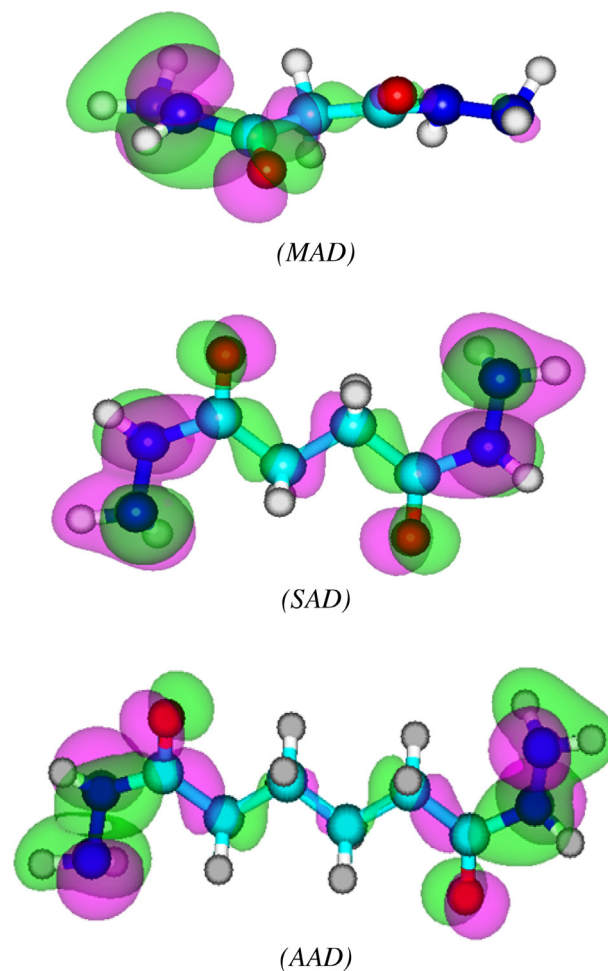


Figure 4 The highest occupied molecular orbital (HOMO) of the inhibitors (I–III).

Table 3 Quantum chemical parameters of the studied inhibitors.

Parameter	MAD	SAD	AAD
E_{HOMO} (eV)	-10.641	-10.141	-9.641
E_{LUMO} (eV)	0.853	0.613	0.373
ΔE (eV)	11.493	10.753	10.015
μ (D)	2.218	2.948	4.876
Vol (\AA^3)	425.985	486.942	582.340
Ar (\AA^3)	295.911	335.987	384.637
V_m (\AA^3)	11.855	13.690	17.360
TE (eV)	-45245	-48838	-56024
χ	4.89	4.764	4.634
σ	0.174	0.1859	0.199

Fig. 4. It is clear that the lower HOMO corresponds to MAD (-10.641 eV) which exhibited the lower inhibition efficiency and the highest value is obtained by AAD (-9.641) which is the best one. The lowest LUMO levels obtained are 0.853, 0.613 and 0.3734 eV; Fig. 5. This can explain that the highest inhibition efficiency of AAD molecule is due to the increasing energy of the HOMO and the decreasing energy of the LUMO. This is in a good agreement with the experimental observations suggesting that the AAD has the highest inhibition efficiency among the investigated inhibitors.

The dipole moment μ is an index, which can also be used for the prediction of the direction of a corrosion inhibition process. Dipole moment is the measure of polarity in a bond and is related to the distribution of electrons in a molecule (Gece, 2008). Although literature is inconsistent on the use of ' μ ' as a predictor for the direction of a corrosion inhibition reaction, it is generally agreed that the adsorption of polar compounds possessing high dipole moments on the metal surface should lead to better inhibition efficiency. Comparison of the results obtained from quantum chemical calculations

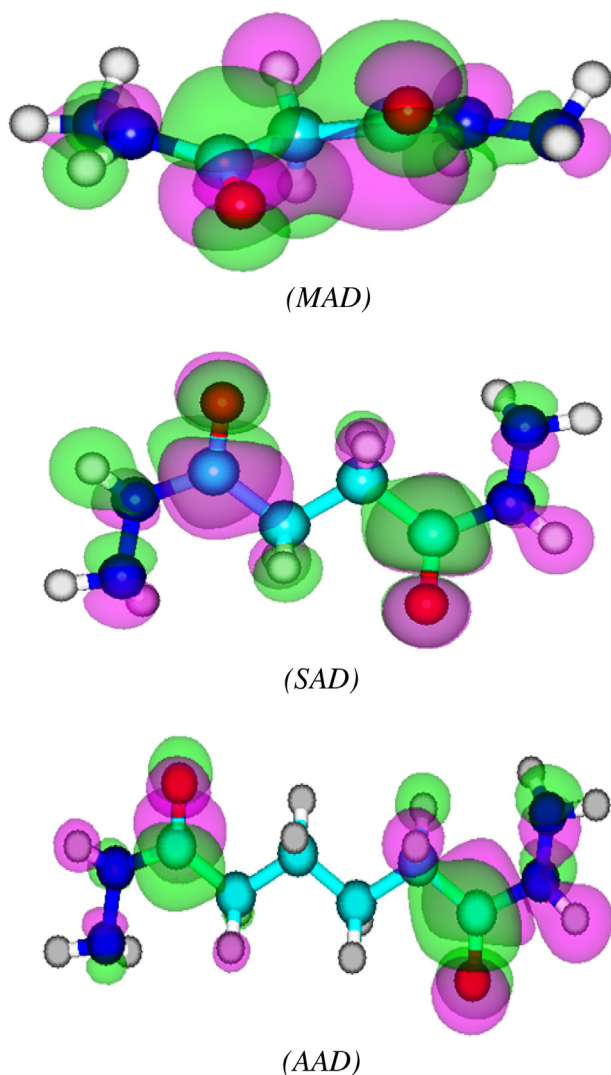


Figure 5 The lowest unoccupied molecular orbital (LUMO) of the inhibitors (I–III).

with experimental inhibition efficiencies indicated that the % inhibition efficiencies of the inhibitors increase with increasing value of the dipole moment.

The estimation of the total energy gives good information, the lower TE obtained is related to MAD which exhibited weaker inhibition. The higher TE ($-56,024$ kcal mol $^{-1}$) confirms the higher stability of AAD.

Polarizability is the ratio of induced dipole moment to the intensity of the electric field. The induced dipole moment is proportional to polarizability (Eddy et al., 2009a,b). Some attempts have been made to relate the polarizability of some corrosion inhibitors to their inhibition efficiency. According to (Arslan et al., 2009), the minimum polarizability principle (MPP) expects that the natural direction of evolution of any system is toward a state of minimum polarizability. From the results obtained from quantum chemical calculations, the trend for the increase in the inhibition efficiencies of the tested inhibitors with respect to increasing polarizability correlates well with the order of the experimental % inhibition efficiency results AAD > SAD > MAD.

The inhibition efficiency of nickel corrosion in 1 M H₂SO₄ solution by dihydrazide derivatives using the above techniques was found to depend on the number of adsorption sites in the molecule and their charge density and molecular size. The inhibition effect of the compounds is attributable to the adsorptions of the inhibitor molecules on the metal surface. The adsorption is assumed to take place mainly by the action of the nitrogen atoms in the dihydrazide compounds (active center).

Terms involving the frontier molecular orbitals could provide dominative contribution, because of the inverse dependence of stabilization energy on orbital energy difference (Fang and Li 2002). Moreover, the gap between the HOMO and LUMO energy levels of the molecules was another important factor that should be considered.

The gap energy, $\Delta E = (E_{\text{LUMO}} - E_{\text{HOMO}})$, is an important parameter as a function of reactivity of the inhibitor molecule toward the adsorption on metallic surface. As ΔE decreases, the reactivity of the molecule increases leading to an increase in the inhibition efficiency of the molecule; and large gap energy indicates high stability of the molecule in the chemical reaction. Fig. 6 shown the diagrams of frontier molecular orbitals for the investigated inhibitors to their estimated energy gap ΔE . Inhibition of corrosion is generally interpreted by

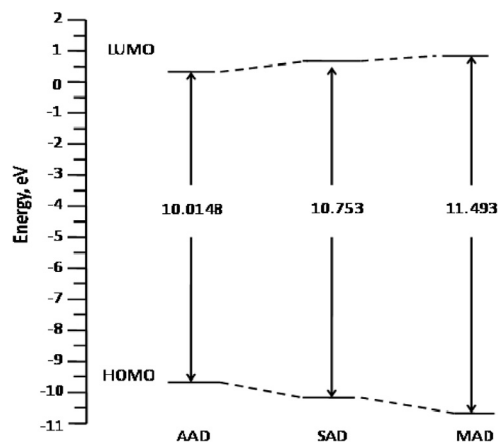


Figure 6 Correlation diagram of frontier molecular orbitals for the investigated inhibitors and their calculated ΔE .

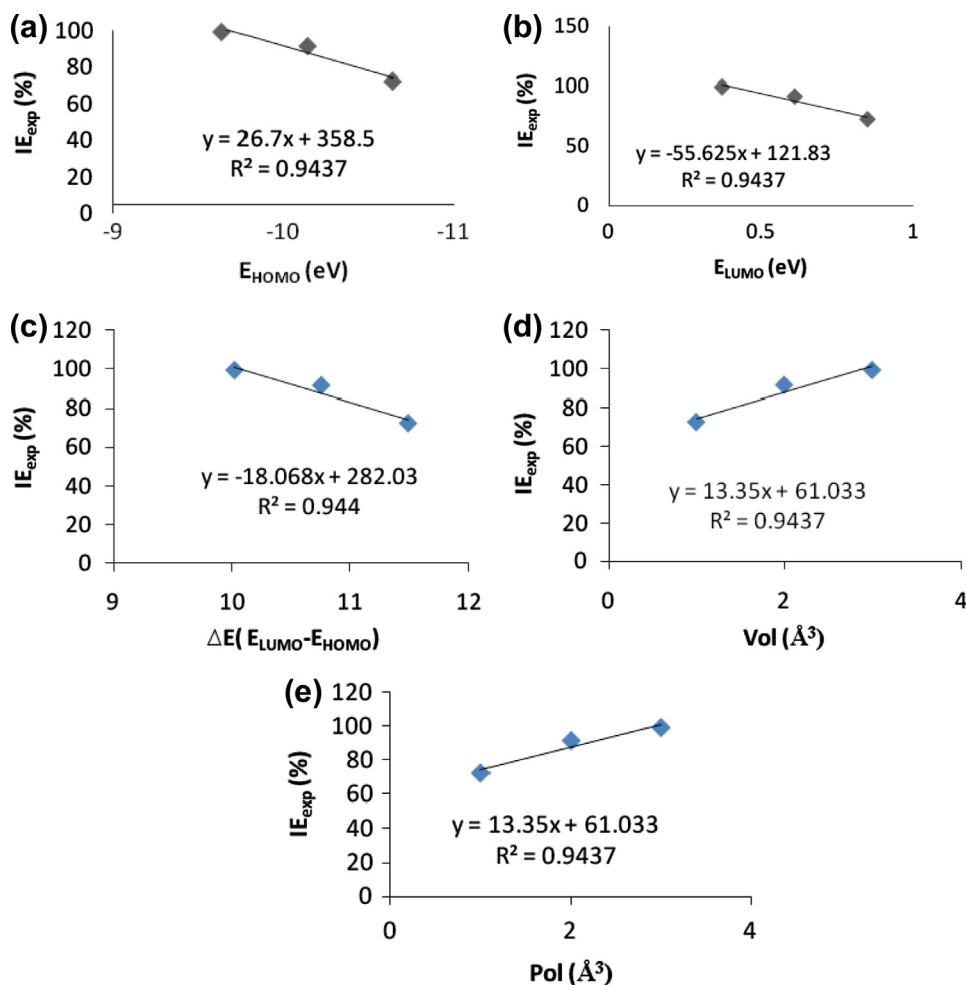


Figure 7 Variation of experimental inhibition efficiency (IE_{exp}) of the studied inhibitors with (a) E_{HOMO} (b) E_{LUMO} (c) $E_{LUMO-HOMO}$ (d) volume and (e) polarizability.

adsorption of inhibitor molecules onto the metal surface. Two modes of adsorption can be envisaged. The physical adsorption requires the interaction of electrically charged metal surface and charged species in the bulk of the solution. Chemisorption mode implies charge sharing or charge transfer from the inhibitor molecule to the vacant orbitals of metal having low energy (Chetouani et al., 2006). Reportedly, excellent corrosion inhibitors are usually those organic compounds who not only offer electrons to unoccupied orbital of the metal, but also accept free electrons from the metal (Gece, 2008).

Correlations between the calculated quantum chemical parameters were also carried out. Fig. 7 shows plots of the variation of the experimental inhibition efficiencies with some quantum chemical parameters. The figure reveals that the degree of linearity R^2 between the plotted quantum chemical parameters and the experimental inhibition efficiencies was very close to unity (≈ 0.94), which indicated a high degree of linearity. From the results obtained, the highest degree of linearity between the experimental inhibition efficiencies and the E_{HOMO} , E_{LUMO} , ($E_{LUMO-HOMO}$), volume (molecular volume) and molecular polarizability (pol), was obtained. However, R^2 values with respect to μ and TE were relatively low (≈ 0.77 , 0.82 respectively).

Other indicators are absolute electronegativity, χ , and absolute hardness η , χ is a chemical property that describes the ability of a molecule to attract an electron toward itself in a covalent bond, while the absolute hardness is measured by the energy gap between the lowest unoccupied and highest occupied molecular orbitals. Absolute softness, σ is defined as the reciprocal of the hardness η , η and σ are calculated using the energies of the HOMO and the LUMO orbitals of the inhibitor molecule and are related to the ionization potential, I , and the electron affinity, A , respectively, by the following relations:

$$X = \frac{I + A}{2}; \eta = \frac{I - A}{2} \quad \text{And} \quad \sigma = \frac{2}{I - A}$$

where

$$I = -E_{HOMO}; \quad A = -E_{LUMO}$$

Values of χ , and η were calculated by using the values of χ , and η obtained from quantum chemical calculation. Using a theoretical χ , value of 4.4 eV/mol according to Pearson's electronegativity scale and η value of 0 eV/mol for nickel (Pearson, 1988). As shown in Table 3 the results deduced indicate that the electron flow will happen from the molecule with low elec-

tronegativity toward that of a higher value, until the chemical potentials are the same. In our case, the best inhibitory effect is shown by AAD with low electronegativity but MAD possesses the higher value.

Several protocols describing selectivity and reactivity by means of orbital Fukui indices are presented by Mineva et al. (2001). The reactivity indices are not directly attained experimentally and only the relative trends between theoretical data and experimental information can be compared and analyzed. With the purpose of having a wider knowledge about the local reactivity of inhibitors, the Fukui indices for each atom in the three inhibitor molecules have been calculated. An analysis of the Fukui indices along with the distribution of charges and the global hardness provides a more complete scheme of the reactivity of the studied molecules (Cruz et al., 2001). The calculated Fukui indices for all the charged species of the three inhibitors ($N + 1$ and $N - 1$) as well as neutral ones (N) are presented in Table 4. For simplicity, only the charges and Fukui functions over the N, O and C atoms were recorded. It has been proven that local electron densities or charges are important in many chemical reactions and physico-chemical properties of compound (Gece, 2008). Fig. 3 shows that all N, O and some of C atoms carry negative charges. This indicates that these atoms are the negative charge centers which could offer electrons to the nickel atoms on the surface to form a coordinate bond.

It is possible to evaluate condensed Fukui functions for nucleophilic, electrophilic, and radical attack from single-point calculations directly, without resorting to additional calculations involving the systems with N , $N - 1$ and $N + 1$ electron and are presented in Table 4.

The resulting change in electron density is the nucleophilic and electrophilic Fukui functions, which can be expressed using the finite difference approximation as follows,

$$f_K^+ = q_{(N+1)} - q_{(N)}$$

$$f_K^- = q_{(N)} - q_{(N-1)}$$

where $q_{(N+1)}$, $q_{(N)}$ and $q_{(N-1)}$ are the Mulliken charge of the atom with $N + 1$, N and $N - 1$ electrons.

Frontier orbital electron densities on atoms provide a useful means for the detailed characterization of donor-acceptor interactions. In the case of a donor molecule, the HOMO density is critical to the charge-transfer (electrophilic electron density f_K^-) and in the case of an acceptor molecule, the LUMO density is important (nucleophilic electron density f_K^+). However, frontier electron densities can strictly be used only to describe the reactivity of different atoms in the same molecule. An analysis of Fukui indices shown in Table 4, demonstrates that, in all cases, the N and O-atoms are the most susceptible sites for electrophilic attacks, these sites present the highest values of f_K^- (Cruz et al., 2001).

Table 4 Calculated Mulliken atomic charges and Fukui functions of inhibitors.

Inhibitor	Atom	$q(N)$	$q(N - 1)$	$q(N + 1)$	f_K^+	f_K^-	f_K^0
MAD	1(C)	0.034685	-0.261789	0.224928	0.190243	0.296474	0.243359
	2(C)	0.170848	0.168747	0.253696	0.082848	0.002101	0.042475
	3(N)	-0.210129	-0.173925	-0.161519	-0.05139	-0.03620	0.006203
	4(N)	0.123475	-0.053837	0.088138	-0.03534	0.177312	0.070988
	5(O)	-0.20155	-0.293696	-0.08984	0.11171	0.092146	0.101928
	6(C)	0.170847	0.162039	0.33986	0.169013	0.008808	0.088911
	7(N)	-0.210111	-0.176694	-0.112798	0.097313	-0.03342	0.031948
	8(O)	0.123476	-0.059218	0.370037	0.246561	0.182694	0.214628
	9(O)	-0.20154	-0.311625	0.087499	0.289039	0.110085	0.199562
SAD	1(C)	0.240241	0.134675	0.280109	0.039868	0.105566	0.072717
	2(C)	0.040684	-0.013745	0.086219	0.045535	0.054429	0.049982
	3(N)	-0.033736	-0.405108	0.121665	0.155401	0.371372	0.263387
	4(N)	0.149058	-0.201367	0.39988	0.250822	0.350425	0.300624
	5(O)	-0.371717	-0.353976	-0.059683	0.152034	-0.01774	0.147147
	6(C)	-0.006809	-0.01365	0.125261	0.13207	0.006841	0.069456
	7(C)	0.260972	0.19394	0.274627	0.013655	0.067032	0.040344
	8(N)	-0.205821	-0.150799	-0.16535	0.040471	-0.05502	-0.00728
	9(N)	-0.018211	-0.016505	0.120637	0.138848	-0.00171	0.068571
	10(O)	-0.214663	-0.173464	-0.183366	0.031297	-0.0412	-0.00495
AAD	1(C)	0.274326	0.181816	0.286606	0.01228	0.092510	0.052395
	2(N)	-0.199798	-0.166419	0.158016	0.357814	-0.03338	0.162218
	3(N)	0.001736	-0.01181	0.261625	0.259889	0.013546	0.136718
	4(O)	-0.28088	-0.184132	-0.000462	0.280418	-0.09675	0.091835
	5(C)	0.274412	0.19488	0.231253	-0.04316	0.079532	0.018187
	6(N)	-0.190758	-0.173847	-0.116323	0.074435	-0.01691	0.028762
	7(N)	0.063319	-0.029093	0.035841	-0.02748	0.092412	0.032467
	8(O)	-0.291239	-0.274904	-0.146473	0.144766	-0.01634	0.064216
	9(C)	-0.194559	-0.157287	0.044623	0.239182	-0.03727	0.100955
	10(C)	0.008969	-0.161933	0.068966	0.059997	0.170902	0.11545
	11(C)	0.008974	-0.14037	0.077043	0.068069	0.149344	0.108707
	12(C)	-0.024503	-0.0769	0.099282	0.123785	0.052397	0.088091

The site for potential nucleophilic attack would depend on the values of f_K^+ on the atoms with a positive charge density. The results from Table 4 show that the site for nucleophilic attack will be the carbon atoms. Finally, the sites for radical attack, governed by the values of f_K^0 will be carbon atom and some of the oxygen atoms.

Table 4 presents values of f_K^+ and f_K^- for inhibitors. As a rule, the respective site for electrophilic and nucleophilic attacks will be the place where the value of f_K^+ or f_K^- is maximum. From the results, it is evident that the site for electrophilic attack in MAD is in N (3), SAD is in N (8) and AAD is in N (2) and O (4) because highest values of f_K^- are found there.

The HOMO and LUMO orbitals of inhibitors are presented in Figs. 4 and 5. These figures clearly reveal the information that governs the nucleophilic and electrophilic attacks on the studied inhibitors. The information obtained from the HOMO and LUMO orbitals are consistent with the findings obtained from the Fukui function.

5. Conclusion

The theoretical study of dihydrazide molecules MAD, SAD and AAD, indicated that all inhibitor systems have a very similar capacity for charge donation, since the values of E_{HOMO} presented a small difference between them. Also the AAD has the lowest value of energy gap and it could have a better performance as corrosion inhibitor. The most efficient inhibitor was the AAD, with an inhibition efficiency of 99.2% whereas the least efficient was the MAD, with an efficiency of 72.5%.

References

- Abdallah, M., Megahed, H.E., Elnager, M.M., Mabrouk, E.M., Radwan, D., 2003. *Bull. Electrochem.* 19, 245.
- Aksut, A.A., Bilgic, S., 1992. *Corros. Sci.* 33, 379.
- Arslan, T., Kandemirli, F., Ebenso, E.E., Love, I., Alemu, H., 2009. *Corros. Sci.* 51, 35.
- Ateya, B.G., Abo El-Khair, M.B., Abdel Hamed, I.A., 1976. *Corros. Sci.* 16, 163.
- Barkalatsova, L.A., Pshenicknikov, A.G., 1976. *Electrochemistry*, 1242.
- Bentiss, F., Lebrini, M., Lagrenee, M., Traisnel, M., Elfarouk, A., Vezin, H., 2007. *Electrochim. Acta* 52, 6865.
- Bouklah, M., Hammouti, B., Benkaddour, M., Benhadda, T., 2005. *J. Appl. Electrochem.* 35, 1095.
- Chetouani, A., Daoudi, M., Hammouti, B., Benhadda, T., Benkaddour, M., 2006. *Corros. Sci.* 48, 2987.
- Cruz, J., Martínez-Aguilera, L.M., Salcedo, R., Castro, M., 2001. *Int. J. Quant. Chem.* 85, 546.
- Dehri, I., Ozcan, M., 2008. *Mater. Chem. Phys.* 98, 316.
- Deng, S.D., Li, X.H., Fu, H.T., 2011. *Corros. Sci.* 53, 822.
- Dewar, M.J.S., Liotard, D.A., 1990. *J. Mol. Struct. (Theochem)* 206, 123.
- Ebenso, E.E., Arslan, T., Kandemirli, F., Caner, N., Love, I., 2010. *Int. J. Quant. Chem.* 110, 1003.
- Eddy, N.O., Ibok, U.J., Ebenso, E.E., El Nemr, A., El Ashry, H.E., 2009a. *J. Mol. Model.* 15, 1085.
- Eddy, N.O., Odoemelam, S.A., Odiongenyi, A.O., 2009b. *J. Appl. Electrochem.* 39, 849.
- Emregul, K.C., Hayvali, M., 2006. *Corros. Sci.* 48, 797.
- Fang, J., Li, J., 2002. *J. Mol. Struct. (Theochem)* 593, 179.
- Feller, H.G., Ratzer Scheibe, H.G., Wendt, W., 1973. *Electrochim. Acta*, 18175.
- Finsgar, M., Lesar, A., Kokajic, A., Milosev, I., 2008. *Electrochim. Acta* 53, 8287.
- Fouda, A.S., Tawfik, H., Abdallah, N.M., Ahmd, A.M., 2013. *Int. J. Electrochem. Sci.* 8, 3390.
- Frignani, A., Monticelli, C., Trabaneli, G., 1998. *Br. Corros. J.* 33, 71.
- Fukui, K., Yonezawa, T., Nagata, C., Shingu, H., 1954. *J. Chem. Phys.* 22, 1433.
- Gatos, H.S., 1956. *Corrosion NACE* 12, 23t-48.
- Gece, G., 2008. *Corros. Sci.* 50, 2981.
- Gomez, B., Likhanova, N.V., Aguilar, M.A.D., Palou, R.M., Vela, A., Gasquez, J.L., 2006. *J. Phys. Chem.* 110, 8928.
- Graz, I., Galzer, B., 1974. *Corros. Sci.* 14, 253.
- Gurten, A.A., Kayakırlmaz, K., Erbil, M., 2007. *Constr. Build. Mater.* 21, 669.
- Hansch, C., Leo, A. (Eds.), 1979. *Correlation Analysis in Chemistry and Biology*, Wiley, New York, NY, USA.
- Hinchliffe, A., 1994. *Modelling Molecular Structures*. John Wiley & Sons, New York.
- Hinchliffe, A., 1999. *Chemical Modelling From Atoms to Liquids*. John Wiley & Sons, New York.
- HyperChem™ Professional 7.5 (Evaluation Version), 2002. Hypercube Inc, Gainesville, FL, USA.
- Issa, R.M., Awad, M.K., Atlam, F.M., 2008. *Appl. Surf. Sci.* 255, 2433.
- Karelson, M., Lobanov, V.S., Katritzky, A.R., 1996. *Chem. Rev.* 96, 1027.
- Kesten, M., 1976. *Corrosion* 32, 94.
- Khaled, K.F., Samardžija, K.B., Hackerman, N., 2005. *Electrochim. Acta* 50, 2515.
- Khamis, E., Bellucci, F., Latanision, R.M., El-Ashry, E.S.H., 1991. *Corrosion* 47, 677.
- Kraka, E., Cremer, D., 2000. *J. Am. Chem. Soc.* 122, 8245.
- Lewis, G., 1982. *Corros. Sci.* 22, 579.
- Luenberger, D.G., 1973. *Introduction to linear and nonlinear programming*, Addison-Wesley, Don Mills, Ont.
- Maayta, A.K., Rawshdeh, N.A.F., 2004. *Corros. Sci.* 46, 1129.
- Maitra, A.M., Bhattacharyya, K., 1979. *J. Ind. Chem. Soc. LVI*, 1202.
- Martinez, S., Valek, L., Stipanović, Oslaković, I., 2007. *J. Electrochem. Soc.* 154, C671.
- Mineva, T., Parvanov, V., Petrov, I., Neshev, N., Russo, N., 2001. *J. Phys. Chem. A* 105, 1959.
- Mohammed, A Amin., Shokry, H., Mabrouk, E.M., 2012. *Corrosion* 68 (8), 699.
- Pang, X., Hou, B., Li, W., Liu, F., Yu, Z.Chin., 2007. *J. Chem. Eng.* 15, 909.
- Pearson, R.G., 1988. *Inorg. Chem.* 27, 734.
- Quraishi, M.A., Ahamad, I., Singh, A.K., Shukla, S.K., Lal, B., Singh, V., 2008. *Mater. Chem. Phys.* 112, 1035.
- Solmaz, Ramazan., 2014. *Corros. Sci.* 79, 169.
- Rengamani, S., Vasudvan, I., Lyer, S.V.K., 1993. *Ind. J. Technol.* 31, 519.
- Reshetnikov, S.M., 1978. *Port. Met.* 14, 491.
- Rodríguez-Valdez, L.M., Martínez-Villafañe, A., Glossman-Mitnik, D., 2005. *J. Mol. Struct. (Theochem)* 713, 65.
- Şahin, M., Gece, G., Karci, F., Bilgiç, S., 2008. *J. Appl. Electrochem.* 38, 809.
- Schmit, G., 1984. *Br. Corros. J.* 19 (4), 465.
- Solomon, M.M., Umoren, S.A., Udoso, I.I., Udoh, A.P., 2010. *Corros. Sci.* 52, 1317.
- Stoyanova, A.E., Peyerimhoff, S.D., 2002. *Electrochim. Acta* 47, 1365.

- Tao, Z., Zhang, S., Li, W., Hou, B., 2010. *Ind. Eng. Chem. Res.* 49, 2593.
- Valdez, L.M.R., Villafane, A.M., Mitnik, D.G., 2005. *J. Mol. Struct. Theochem.* 716, 61.
- Valdez, L.M.R., Villamizar, W., Casales, M., Rodriguez, J.G.G., Villafane, A.M., Martinez, L., Mitnik, D.G., 2006. *Corros. Sci.* 48, 4053.
- Wolinski, K., Hinton, J.F., Pulay, P., 1990. *J. Am. Chem. Soc.* 112, 8251.
- Xia, S., Qiu, M., Yu, L., Liu, F., Zhao, H., 2008. *Corros. Sci.* 50, 2021.
- Yang, W., Mortier, W.J., 1986. *J. Am. Chem. Soc.* 108, 5708.
- Zhao, T., Mu, G., 1999. *Corros. Sci.* 41, 1937.
- Zinola, C.F., Castro Luna, A.H., 1995. *Corros. Sci.* 37, 1919.